BJP British Journal of Pharmacology

DOI:10.1111/j.1476-5381.2012.01974.x
www.brjpharmacol.org

RESEARCH PAPER

Modulation of PAR_1 signalling by benzimidazole compounds

S Asteriti[1]*, S Daniele[1]*, F Porchia[1], MT Dell' Anno[1], A Fazzini[1], I Pugliesi[2], ML Trincavelli[1], S Taliani[2], C Martini[1], MR Mazzoni[1] and A Gilchrist[3]

[1]*Department of Psychiatry, Neurobiology, Pharmacology and Biotechnology, University of Pisa, Italy,* [2]*Department of Pharmaceutical Sciences, University of Pisa, Italy, and* [3]*Department of Pharmaceutical Sciences, Midwestern University, IL, USA*

Correspondence
Dr Annette Gilchrist, Department of Pharmaceutical Sciences, Midwestern University, 555 31st Street, Downers Grove, IL 60515, USA. E-mail: agilch@midwestern.edu

*These authors contributed equally to this work.

Keywords
allosteric; benzimidazole scaffold; biased signalling; endothelial cells; functional selectivity; Gα; GPCR; HMEC-1; PAR_1; positive/negative modulation; protease-activated receptor; Q94; thrombin; thrombin receptor

Received
26 January 2011
Revised
14 February 2012
Accepted
19 March 2012

BACKGROUND AND PURPOSE

Recently, a small molecule (Q94) was reported to selectively block $PAR_1/G\alpha_q$ interaction and signalling. Here, we describe the pharmacological properties of Q94 and two analogues that share its benzimidazole scaffold (Q109, Q89). Q109 presents a modest variation from Q94 in the substituent group at the 2-position, while Q89 has quite different groups at the 1- and 2-positions.

EXPERIMENTAL APPROACH

Using human microvascular endothelial cells, we examined intracellular Ca^{2+} mobilization and inositol 1,4,5-trisphosphate accumulation as well as isoprenaline- or forskolin-stimulated cAMP production in response to thrombin.

KEY RESULTS

Q89 (10 μM) produced a leftward shift in the thrombin-mediated intracellular Ca^{2+} mobilization concentration–response curve while having no effect on the E_{max}. Both Q94 (10 μM) and Q109 (10 μM) reduced intracellular Ca^{2+} mobilization, leading to a decrease in E_{max} and an increase in EC_{50} values. Experiments utilizing receptor-specific activating peptides confirmed that Q94 and Q109 were selective for PAR_1 as they did not alter the Ca^{2+} response mediated by a PAR_2 activating peptide. Consistent with our Ca^{2+} results, micromolar concentrations of either Q94 or Q109 significantly reduced thrombin-induced inositol 1,4,5-trisphosphate production. Neither Q94 nor Q109 diminished the inhibitory effects of thrombin on cAMP production, indicating they inhibit signalling selectively through the G_q pathway. Our results also suggest the 1,2-disubstituted benzimidazole derivatives act as 'allosteric agonists' of PAR_1.

CONCLUSIONS AND IMPLICATIONS

The Q94 and Q109 benzimidazole derivatives represent a novel scaffold for the development of new PAR_1 inhibitors and provide a starting point to develop dual signalling pathway-selective positive/negative modulators of PAR_1.

Abbreviations

AP, activating peptide; DAG, diacylglycerol; DMSO, dimethyl sulfoxide; E_{max}, maximal effect; Fluo 3-AM, 1-[2-amino-5-(2,7-dichloro-6-hydroxy-3-oxo-9-xanthenyl)phenoxy]-2-(2-amino-5-methylphenoxy)ethane-*N*,*N*,*N*′,*N*′-tetraacetic acid, pentaacetoxymethyl ester; FSK, forskolin; Gα, the α subunit of heterotrimeric G-proteins; HMEC-1, human dermal microvascular endothelial cell line; IP_3, inositol 1,4,5-trisphosphate; PAR, protease-activated receptor; PTX, pertussis toxin; Ro 20–1724, 4-(3-butoxy-4-methoxyphenyl)methyl-2-imidazolidone; ROC, receptor-operated Ca^{2+} channels; SCH 79797, N3-cyclopropyl-7-[[4-(1-methylethyl)phenyl]methyl]-7h-pyrrolo[3,2-f]quinazoline-1,3-diamine dihydrochloride; SOC, store-operated Ca^{2+} channels; TL, tethered ligand

Introduction

Protease-activated receptors (PARs) are a family of four GPCRs (PAR_1, PAR_2, PAR_3, and PAR_4; receptor nomenclature follows Alexander *et al.*, 2011) characterized by a unique mechanism of activation. PARs are activated enzymatically through proteolysis of the receptor by enzymes of the serine protease family (Macfarlane *et al.*, 2001). The proteolytic cleavage occurs at specific sites within their N-terminal region, thereby exposing novel N-termini, and the 'tethered ligand' then folds back onto the extracellular loop II of the receptor, resulting in activation. PAR_1, PAR_3, and PAR_4 are preferentially cleaved by thrombin; whereas PAR_2 is mainly a substrate for trypsin, and mast cell tryptase (Coughlin, 2001; Macfarlane *et al.*, 2001; Hollenberg and Compton, 2002). In addition to proteolytic cleavage, most PARs can be activated by synthetic peptides corresponding to the tethered ligand (TL) sequence (Ramachandran and Hollenberg, 2008).

PARs are expressed in many cell types and different organ systems. For example, PAR_1, PAR_2, PAR_3 and PAR_4 are all expressed on human endothelial cells (Ramachandran and Hollenberg, 2008); although PAR_4 expression may be localized to the endothelium of specific vascular areas (O'Brien *et al.*, 2000; Fujiwara *et al.*, 2005; Hirano *et al.*, 2007). Upon activation, PAR_1 exerts its effects on endothelium by activating multiple G-proteins, including $G_{i/o}$, $G_{q/11}$ and $G_{12/13}$, leading to modulation of numerous downstream signalling pathways (Barr *et al.*, 1997; Vanhauwe *et al.*, 2002; Ramachandran and Hollenberg, 2008). While PAR_1 expression is widely distributed among cells and tissues, PAR_2 expression is more limited, and studies indicate that signalling occurs via $G_{q/11}$, $G_{i/o}$ (Nystedt *et al.*, 1995; Macfarlane *et al.*, 2001) and perhaps $G_{12/13}$ (Ramachandran *et al.*, 2009).

PAR activation plays a key role in many physiological and pathophysiological events involving different organ systems (Ramachandran and Hollenberg, 2008). For example, in the cardiovascular and circulatory systems, activation of PAR_1 and to a lesser extent PAR_4 on human platelets is sufficient to trigger aggregation (Kahn *et al.*, 1999), while activation of human endothelial PAR_1 and PAR_2 causes vascular relaxation (Hamilton *et al.*, 2001; 2002; Robin *et al.*, 2003). Indeed, PAR antagonists might prove useful therapeutically for the treatment of several diseases, including thrombosis and atherosclerosis.

Several peptide, peptidomimetic and non-peptide PAR_1 antagonists are currently available for experimental studies; and a number of synthetic small molecules are being evaluated for pharmaceutical use in humans (reviewed by Chackalamannil, 2006). In addition, alternative approaches to inhibit PAR_1 signalling, such as transfection of endothelial cells with minigene vectors expressing Gα carboxyl (C)-terminal peptides (Gilchrist *et al.*, 2001), or the use of membrane-permeable peptides termed 'pepducins' derived from the sequence of the third intracellular loop of PAR_1 (Covic *et al.*, 2002a,b), have been presented. Deng *et al.* (2008) reported the use of a small molecule, Q94, which selectively blocks the interaction between PAR_1 and $G\alpha_q$, to investigate thrombin mediated signalling in mouse lung fibroblasts. Q94 was originally identified during an ELISA screen for competition of a high-affinity peptide mimicking the C-terminus of $G\alpha_q$ using a compound library (Deng *et al.*, 2008), and the compound may act as a negative allosteric modulator of PAR_1 rather than an orthosteric antagonist. Although Q94 has not been extensively investigated, it represents the first compound to show selective modulation of PAR_1/G-protein interactions and thus serve as a biased inhibitor of thrombin-mediated G_q pathway signalling events.

In the present study, we examined the pharmacological properties of Q94 and two analogues, Q109 and Q89, using human microvascular endothelial cells. The three small molecules (Q94, Q109, Q89) all share a benzimidazole scaffold and present either a modest variation in the substituent group at the 2-position (Q109 vs. Q94) or quite different groups at the 1- and 2-positions (Q89 vs. Q94). Whereas micromolar concentrations of Q94 or Q109 resulted in a 30–50% reduction of thrombin's maximal effect (E_{max}) on intracellular Ca^{2+} mobilization in combination with a two- to threefold increase of thrombin's EC_{50} value, a micromolar concentration of Q89 produced a shift to the left in thrombin's concentration–response curve and had no effect on thrombin E_{max}. Similar to the Ca^{2+} mobilization studies, experiments assessing inositol-1,4,5-trisphosphate (IP_3) accumulation indicated that the presence of micromolar concentrations of either Q94 or Q109 resulted in a significant decrease in thrombin's maximal stimulation (E_{max}). The antagonistic properties of Q94 and Q109 appear selective as they affected the concentration–response curve of a selective PAR_1 activating peptide (AP) while not altering that of a selective PAR_2-AP. In addition, these benzimidazole derivatives did not reverse the inhibitory effect of thrombin on isoprenaline- or forskolin-stimulated cAMP production, suggesting they can selectively inhibit the G_q pathway. Importantly, our studies reveal that although the benzimidazole derivatives Q94 and Q109 behave as selective modulators of PAR_1 signalling and represent a novel scaffold for the development of new PAR_1 inhibitors, their effect on PAR_1 signalling is more complex than simple inhibition of G_q activation.

Methods

Cell culture

Human dermal microvascular endothelial cells (HMEC-1), a generous gift of Dr E Ades (Centers for Disease Control, Atlanta, GA) were grown in MCDB 131 medium supplemented with 5% FBS, penicillin/streptomycin (100 $U \cdot mL^{-1}$; 100 $\mu g \cdot mL^{-1}$), hydrocortisone (1 $\mu g \cdot mL^{-1}$), EGF (0.01 $\mu g \cdot mL^{-1}$) and L-glutamine (2 mM) in an atmosphere of 95% air, 5% CO_2 at 37°C. Cells were seeded at 1×10^5 cells$\cdot mL^{-1}$ in 75 mL cell culture flasks coated with 1% gelatin and subcultured after detachment with 0.05% trypsin, 0.5 mM EDTA. For all of the experiments described, cells were used at passages 17–22.

$[Ca^{2+}]_i$ measurement

Variations in $[Ca^{2+}]_i$ were measured using a Wallac 1420 multilabel counter microplate reader (PerkinElmer, Inc., Waltham, MA) on HMECs-1 loaded with the Fluo 3-AM. HMECs-1 were seeded in black/clear-bottomed 96-well assay plates coated with 1% gelatin at a density of 3×10^4 cells per well and after attachment (6–8 h) were deprived of serum

(serum-starved) for 3 h. Before the start of the assay, cells were washed twice with loading buffer (20 mM HEPES, pH 7.4, 130 mM NaCl, 5 mM KCl, 2 mM $CaCl_2$, 1 mM $MgSO_4$, 0.83 mM Na_2HPO_4, 0.17 mM NaH_2PO_4) containing 25 mM mannose, 1 mg·mL^{-1} BSA and 2.5 mM probenecid and then incubated in 100 µL of the same buffer containing 6 µM Fluo 3-AM/0.024% pluronic acid. After 1 h at 37°C, cells were washed twice with loading buffer and incubated in 100 µL of the same buffer for an additional 1 h at 37°C to remove any excess dye. Fluorescence measurements, reflecting the increase of $[Ca^{2+}]_i$, were carried out at 37°C with an excitation wavelength of 480 nm and emission recorded at 530 nm. Fluorescence was first recorded at baseline and within 20 s of agonist (thrombin, trypsin, PAR_1- or PAR_2-AP) addition. In time course experiments, fluorescence was recorded at baseline and then every 3 s after thrombin (50 nM) addition for another 120 s. The basal intracellular Ca^{2+} concentration was calculated using the following equation based on fluorescence intensity (F):

$$[Ca^{2+}]_i = K_D(F - F_{min})/(F_{max} - F)$$

using $K_D = 390$ nM for Fluo 3. F_{max} was the maximal Ca^{2+} response obtained after cell permeabilization with 20 µM ionomycin for 10 min, while F_{min} was the minimal Ca^{2+} response measured 10 min after addition of 2 mM $MnCl_2$.

Unless otherwise noted, for experiments directed at testing the effects of Q94, Q109 or Q89, the compounds were added 15 min before the addition of agonists. For a series of Ca^{2+} experiments, we added the agonist immediately following the addition of the compounds. Thrombin and trypsin concentration–response curves were performed using up to seven different concentrations of the enzymes (0.01 nM to 1 µM) in the presence and absence of fixed concentrations of PAR_1 modulators (Q94, Q109 or Q89). PAR-AP concentration–response curves were obtained using up to seven different concentrations of activating peptides (0.1–300 µM) in the presence and absence of fixed concentrations of PAR_1 modulators (Q94 or Q109). The concentration–response curves of Q94, Q109 or SCH 79797 were carried out using six different concentrations of the PAR_1 modulators (0.1 nM to 10 µM) at a thrombin concentration of 50 nM. Stock solutions (10 mM) of the compounds were prepared in dimethyl sulfoxide (DMSO) and then diluted in loading buffer. In each well, the concentration of DMSO never exceeded 0.1%, a level at which assay measurements were not affected, as demonstrated by control experiments carried out in the presence of this same concentration of compound vehicle (data not shown). Before the stock solutions were prepared, the structural identity of each compound was verified by routine NMR spectra recorded in d_6-DMSO solution on a Gemini 200 spectrometer (Varian Inc, Santa Clara, CA) operating at 200 MHz (data not shown).

Measurement of intracellular IP_3 levels

Intracellular IP_3 levels were measured using a competitive protein binding method, as previously reported (Gerwins, 1993). Thrombin concentration–response curves were obtained by incubating cells at 37°C for 15 min with different agonist concentrations ranging from 0.1 to 100 nM. To evaluate the effect of compound Q94 and Q109 on IP_3 production, cells were exposed to compound concentrations of 1 or 10 µM in the presence of different thrombin concentrations (15 min at 37°C). Compounds and thrombin were added at the same time. The reaction was terminated by the removal of the medium and the addition of 1 N HCl. After 30 min, lysates were neutralized with 2 N KOH, 1 M Tris and 60 mM EGTA; and the suspension centrifuged at 3000 × g for 10 min.

The binding assay was performed in a 96-well microtitre plate format using a binding protein purified from bovine adrenal gland according to the method published by Gerwins (1993). In this protocol, each well contains 25 µL of assay buffer (100 mM Tris–HCl, pH 9, 4 mM EDTA, 4 mM EGTA, 4 mg·mL^{-1} BSA), 25 µL of [^{3}H]-IP_3 (3000–3500 cpm), 25 µL of binding protein (~0.5 mg) and 25 µL of standard IP_3 (0.02–6.25 pmol) or sample. After 1 h incubation at 4°C, bound [^{3}H]-IP_3 is separated by rapid filtration through GF/C glass fibre filters using a cell harvester. The radioactivity is then measured by liquid scintillation spectrometry.

Measurement of intracellular cAMP

Intracellular cAMP levels were measured using a competitive protein binding method, as previously described (Nordstedt and Fredholm, 1990; Colotta *et al.*, 2009). Cells (4 × 10^4 per well) were plated in 24-well plates in 0.5 mL of medium. After 24 h, the medium was removed; and 0.5 mL of serum free medium with PDE inhibitor, Ro 20–1724 (20 µM), was added and the cells incubated at 37°C for 15 min. Cells were then exposed to different compound concentrations ranging from 100 nM to 10 µM in the presence and absence of 50 nM thrombin (15 min at 37°C). Assays were initiated by the addition of 0.5 µM FSK or 1 µM isoprenaline. The reaction was terminated by the removal of the medium and the addition of 0.4 N HCl. After 30 min, lysates were neutralized with 4 N KOH, and the suspension centrifuged at 800 × g for 5 min. To measure cAMP production, bovine adrenal cAMP binding protein was incubated with [^{3}H]-cAMP (2 nM) and 50 µL of cell lysate or cAMP standard (0–16 pmol) at 0°C for 150 min in a total volume of 300 µL. Bound radioactivity was separated by rapid filtration through GF/C glass fibre filters, and then the filters were washed twice with 4 mL of 50 mM Tris–HCl, pH 7.4. The radioactivity was measured by liquid scintillation spectrometry.

For studies involving pertussis toxin (PTX) (to ADP-ribosylate G_i-proteins), HMEC-1 cells were incubated overnight in serum-free culture medium in the presence or absence of 200 ng·mL^{-1} PTX. These cells were then used to measure FSK-stimulated cAMP production and inhibition by thrombin as described above.

Immunoblot detection of PAR_1 on cell membranes

HMECs-1 were incubated in the presence and absence (control) of 10 µM Q94 or Q109 for 15 min at 37°C. After incubation, cells were rinsed with Dulbecco's PBS (8.1 mM Na_2HPO_4, 1.5 mM KH_2PO_4, pH 7.4, 137 mM NaCl and 2.7 mM KCl) and lysed in hypotonic buffer (5 mM Tris, pH 7.4, 2 mM EDTA and 1 µL·mL^{-1} protease inhibitor cocktail). Cell lysates were centrifuged at 48 000 × g for 30 min at 4°C. Membrane fraction was re-suspended in solubilizing buffer (50 mM Tris, pH 7.4, 150 mM NaCl, 2 mM EGTA, 1% Triton and 1 µL·mL^{-1} protease inhibitor cocktail).

Solubilized proteins were treated with Laemmli solution, boiled for 5 min and then resolved by SDS-PAGE (10% gel). Proteins were then transferred to nitrocellulose membranes, blocked and then probed overnight at 4°C with a rabbit anti-PAR_1 polyclonal antibody (1:200). Following three 5 min washes, the membranes were incubated with an anti-rabbit peroxidase-labelled secondary antibody (1:10 000). The proteins were visualized using enhanced chemiluminescence substrate (Western Lightning® Plus-ECL). If noted, membranes were stripped and re-probed with a mouse anti-β-actin monoclonal antibody (1:2000) for 2 h at room temperature followed by an anti-mouse peroxidase-labelled secondary antibody (1:2000).

Data analysis

Data from concentration–response curves were analysed using GraphPad Prism (version 4.00) for Windows (GraphPad Software, San Diego, CA), to yield EC_{50}, IC_{50} and E_{max} values. Values represent the means ± SEM of at least three independent experiment (n = number of experiments). The statistical analysis was performed by Student's unpaired t-test or one-way ANOVA followed by Bonferroni's multiple comparison test using GraphPad Prism.

Materials

Penicillin, streptomycin, trypsin, hydrocortisone, ionomycin, FSK, cAMP, Ro 20–1724, probenecid, protease inhibitor cocktail and secondary antibodies were products from Sigma-Aldrich Inc. (St. Louis, MO); while [^{3}H]-cAMP (specific activity, 31.0 Ci mmol^{-1}), [^{3}H]-IP_3 (specific activity, 21.5 Ci mmol^{-1}) and enhanced chemiluminescence substrate (Western lightning® Plus-ECL) were from PerkinElmer Inc. (Waltham, MA). MCDB 131 medium, FBS, EGF, L-glutamine, Fluo 3 acetoxy methylester (Fluo 3-AM), pluronic acid and nitrocellulose membrane were purchased from Invitrogen Corporation (Carlsbad, CA). Isoprenaline was from Research Biochemical International (Natick, MA). Human α-thrombin (specific activity, ≥2800 NIH U mg^{-1} protein), PTX and IP_3 were from Calbiochem-Novabiochem Corp. (San Diego, CA). PAR_1-AP, TFLLR-NH_2 and PAR_2-AP, SLIGRL-NH_2, were synthesized by Espikem s.r.l. (Florence, Italy). Q89, Q94 and Q109 were synthesized on site but can be ordered from ChemDiv (San Diego, CA) as compound numbers 1774-0089, 5786-1094 and C147-0109, respectively. SCH 79797 was purchased from Tocris Bioscience (Bristol, UK). Primary antibodies were from Santa Cruz Biotechnology Inc (Santa Cruz, CA). Other agents and reagents were from standard commercial sources and were of the highest grade available.

Results

Effects of PAR agonists on intracellular Ca^{2+} mobilization

Human endothelial cells express all four PARs (Ramachandran and Hollenberg, 2008), although PAR_4 expression may be restricted to the endothelium of specific vascular areas (O'Brien *et al.*, 2000; Fujiwara *et al.*, 2005; Hirano *et al.*, 2007). HMEC-1, a dermal microvascular cell line established in 1992 (Ades *et al.*, 1992) has proven to be a useful tool for endothelial cell studies. McLaughlin *et al.* (2005) reported that PAR_4 is not expressed in this cell line. In order to test the ability of the benzimidazole compounds to selectivity modulate PAR_1 versus PAR_2 signalling in HMEC-1, we measured receptor-induced G_q activation and subsequent intracellular Ca^{2+} mobilization using PAR-APs and compared results with those obtained following thrombin or trypsin stimulation. Two agonist peptides, TFLLR-NH_2 and SLIGRL-NH_2, were used to selectively activate PAR_1 and PAR_2, respectively (Luo *et al.*, 2007; Ramachandran and Hollenberg, 2008).

To measure Ca^{2+} transients, we utilized Fluo 3-AM and a Wallac 1420 multilabel counter microplate reader, as described under Methods. Thrombin, trypsin and selective PAR-APs induced rapid and transient increases in $[Ca^{2+}]_i$ in a concentration-dependent manner (Figure 1A and B). Saturating amounts of either thrombin or trypsin produced an approximately twofold increase of $[Ca^{2+}]_i$. Thrombin mobilized intracellular Ca^{2+} with an EC_{50} of 8.4 ± 0.8 nM (n = 4), while the EC_{50} for trypsin was 6.8 ± 0.7 nM (n = 6) (Figure 1A). The EC_{50} value for thrombin-induced intracellular Ca^{2+} mobilization was approximately fivefold higher than that reported by McLaughlin *et al.* (2005) in the same endothelial cell line. However, we must point out that our assay conditions and fluorescence detection system were quite different from those previously described. PAR_1-AP and PAR_2-AP induced similar, substantial elevations in $[Ca^{2+}]_i$ in a concentration-dependent manner (Figure 1B). Saturating concentrations (300 μM) of each agonist peptide caused an approximately two- to threefold increase in $[Ca^{2+}]_i$, with EC_{50} values of 6.7 ± 0.8 μM (n = 6) for PAR_1-AP and 11.4 ± 0.8 μM (n = 6) for PAR_2-AP. Thus, thrombin, trypsin, PAR_1-AP and PAR_2-AP were all found to induce Ca^{2+} mobilization responses.

Modulation of PAR-induced intracellular Ca^{2+} mobilization by benzimidazole derivatives

Here, we examined the pharmacological properties of Q94 as well as two other compounds, Q89 and Q109, which share the Q94 benzimidazole scaffold. Q89 and Q109, like Q94, compete with a high-affinity peptide mimic of the $G\alpha_q$ C-terminus (Supplementary Data S1; Figure S1). Both Q94 and Q109 bear a *p*-chlorobenzyl moiety at the 1-position of the benzimidazole scaffold, but at the 2-position, they differ in the flexibility of the side chains ending with a benzyl group (Figure 4). On the other hand, Q89 bears quite different groups at the 1- and 2-positions as compared with those of Q94 and Q109 (Figure 4). In our initial experiments, we tested the effect of either 1 μM Q94 or Q109 on Ca^{2+} transient induced by HMEC-1 stimulated with 50 nM thrombin, a concentration that provides maximal Ca^{2+} mobilization. The resulting traces (Figure 2A and B) indicate that in the first 15 s, both compounds significantly reduced the $[Ca^{2+}]_i$ increase irrespective of the time of their addition. Furthermore, pre-incubation of HMECs-1 in the presence of either Q94 or Q109 did not modify PAR_1 amounts on the cell membrane, as shown using immunoblot analysis followed by densitometric scanning (Figure 2C). Next, we varied the concentration of thrombin and looked at the effect of fixed concentrations of the benzimidazole compounds on thrombin-induced intracellular Ca^{2+} mobilization.

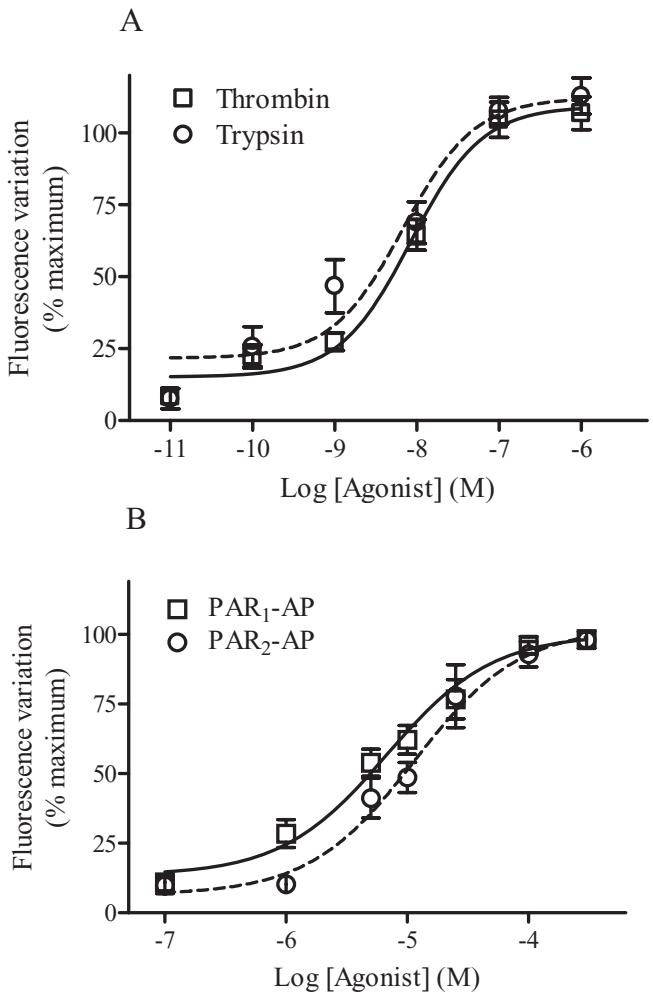

Figure 1

Concentration-dependent intracellular Ca^{2+} mobilization by PAR_1 and PAR_2 agonists (A, activating proteases; B, PAR-APs). Intracellular Ca^{2+} mobilization was measured using Fluo 3-AM-loaded HMECs-1 as described in Methods. Basal $[Ca^{2+}]_i$, calculated as described in Methods, was 255.7 ± 39.3 nM ($n = 8$). Data are reported as % of maximal relative fluorescence (RF) (RF = ($F_s - F_0$) / F_0, where F_0 is basal fluorescence, and F_s is fluorescence recorded after cell stimulation with the agonist) and are the means ± SEM of four (A) and six (B) independent experiments, each performed in triplicate.

Q94 altered the concentration–response curve of thrombin. Specifically, at low thrombin concentrations (10 pM to 1 nM), 100 nM Q94 produced a conspicuous increase in the fluorescent signal, indicating an increase in $[Ca^{2+}]_i$, while at higher enzyme concentrations the same amount of Q94 (100 nM) resulted in a decrease in thrombin E_{max} when compared to a control concentration–response curve with an E_{max} value of 71.9 ± 4.8% ($n = 3$) (Figure 3A; Table 1). Under these conditions, Q94 caused an approximately fourfold decrease in thrombin EC_{50} value. However, when Q94 was used at higher concentrations (1 and 10 μM), no increase in $[Ca^{2+}]_i$ was observed at low thrombin concentrations. Rather, rightward shifts in the thrombin concentration–response curve with an approximately twofold increase in EC_{50} value and ~30% decrease in the maximal response (Figure 3A; Table 1) were observed.

An increase in $[Ca^{2+}]_i$ was also demonstrated with 100 nM Q109, but unlike Q94, the thrombin concentration–response curve was not altered, although the calculated EC_{50} value was modestly increased (Figure 3B). As seen with Q94, when used at 1 or 10 μM concentrations, Q109 resulted in shifts to the right of the curve with a two- to threefold increase in thrombin EC_{50} values (Figure 3B; Table 1). In addition, as was observed with Q94, Q109 also decreased thrombin's maximal response, with E_{max} values of 84.2 ± 7.4% ($n = 4$) and 62.0 ± 2.6% ($n = 4$) in the presence of 1 and 10 μM, respectively. The rightward shift in thrombin's response curve along with the decreased E_{max} values support the hypothesis that the benzimidazole derivatives Q94 and Q109 behave as allosteric modulators of PAR_1.

The third benzimidazole derivative, compound Q89, did not cause either a decrease in thrombin E_{max} or an increase in the EC_{50} value when given at a concentration of 10 μM. Rather, it steepened the concentration–response curve of the agonist leading to an approximately threefold decrease in the EC_{50} value (Figure 4, inset; Table 1). Although a steepening of the concentration–response curve is indicative of an interaction that is not simply competitive, this compound was not further tested due to its lack of inhibitory activity on thrombin E_{max}.

Next, we addressed the potency of Q94 and Q109 as inhibitors of thrombin-induced intracellular Ca^{2+} mobilization by performing concentration–response curves for the compounds at a fixed concentration of thrombin (50 nM). This thrombin concentration was selected as it provided a consistent level of fluorescence signal. We compared the potency of Q94 and Q109 with that of a commercially available PAR_1 antagonist, SCH 79797. All three compounds inhibited thrombin-mediated $[Ca^{2+}]_i$ increases in a concentration-dependent fashion (Figure 5). The IC_{50} values for Q94, Q109 and SCH 79797 inhibitions were 10.3 ± 0.7 nM ($n = 3$), 19.2 ± 0.6 nM ($n = 3$) and 50.6 ± 0.6 nM ($n = 3$), respectively. The IC_{50} value obtained for SCH 79797 was similar to the IC_{50} value reported for inhibition of thrombin-induced Ca^{2+} transient in vascular smooth muscle cells (Ahn *et al.*, 2000). Interestingly, whereas SCH 79797 concentrations ranging between 0.1 and 1 nM caused a ~25% inhibition of fluorescence variation, the same concentrations of either Q94 or Q109 induced an increase in fluorescence (Figure 5). In the absence of agonist, the benzimidazole derivatives had no significant effect on basal fluorescence (Figure 5), indicating the observed differences were not the result of intrinsic fluorescence.

To determine whether Q94 and Q109 benzimidazole derivatives were subtype-selective, we investigated their effects on PAR_1-AP- and PAR_2-AP-induced intracellular Ca^{2+} mobilization. In the presence of either 1 or 10 μM Q94, the PAR_1-AP concentration–response curves were shifted to the right with an approximately twofold increase in EC_{50} values being observed when compared with the control EC_{50} value (Figure 6A; Table 1). Moreover, while 1 μM Q94 did not cause a significant decrease in the PAR_1-AP E_{max} value, 10 μM Q94 resulted in a 28% reduction in the maximal response. The concentration–response curve for PAR_2-AP was not affected by the addition of either 1 or 10 μM Q94, indicating the compound is not a modulator of PAR_2 signalling to

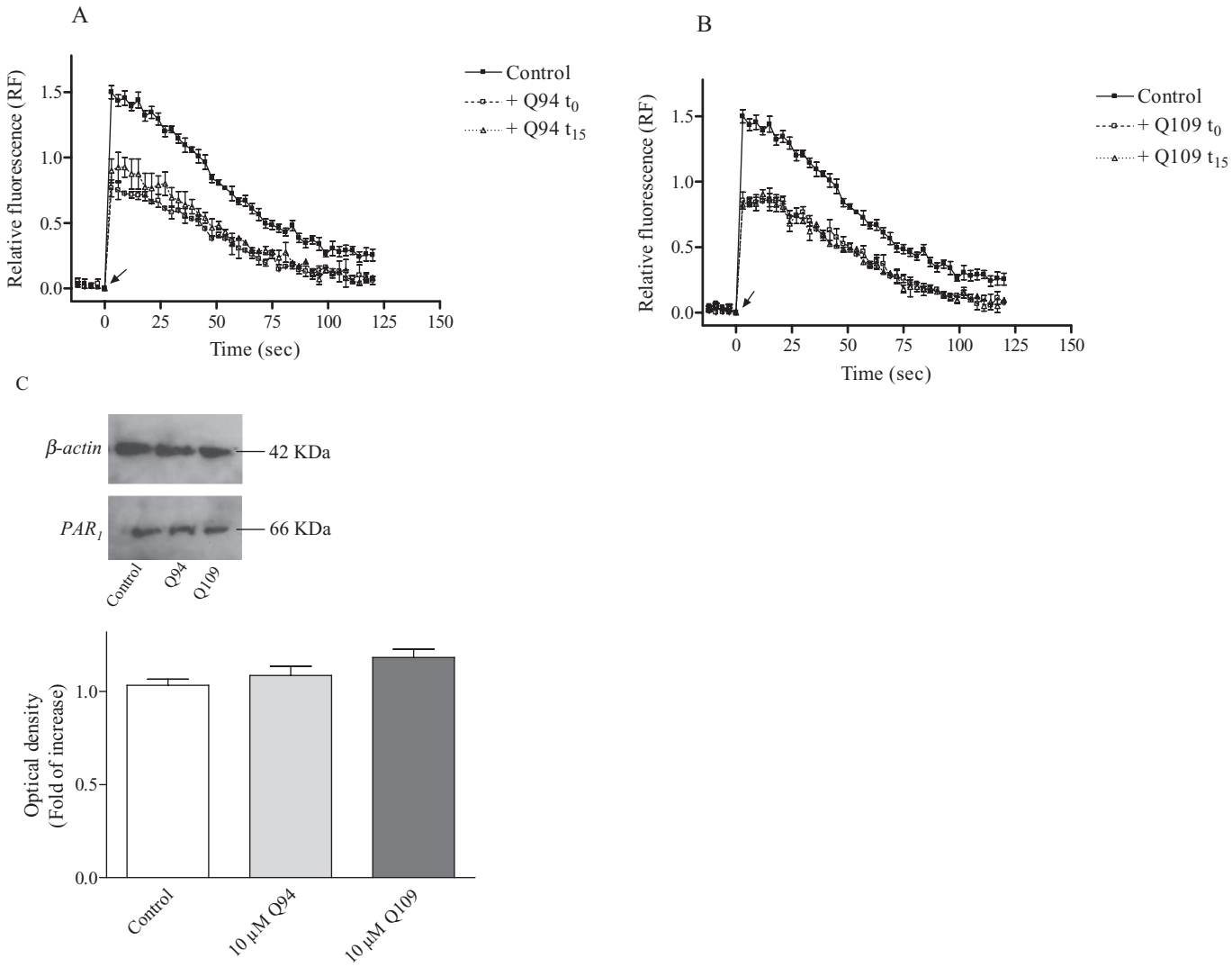

Figure 2

Effect of Q94 and Q109 on $[Ca^{2+}]_i$ transients in HMECs-1 in response to thrombin (A and B) and PAR_1 levels on cell membrane (C). (A and B) Intracellular Ca^{2+} was measured using Fluo 3-AM-loaded HMECs-1 as described in Methods. Fluorescence was recorded before and then every 3 s after 50 nM thrombin addition for 120 s. The benzimidazole compounds (1 μM) were added immediately before, or 15 min before, thrombin addition. Values, reported as RF, are the means ± SEM of three independent experiments, each performed in triplicate. In the first 15 s after thrombin addition, RF values in the presence of compounds are significantly different form those obtained in the absence (control) ($P < 0.01$ and $P < 0.001$) as determined by ANOVA followed by Bonferroni's multiple comparison test. The arrows indicate addition of thrombin. (C) Solubilized membrane proteins were subjected to SDS-PAGE and electroblotted. A rabbit anti-PAR_1 polyclonal antibody was used in immunoblots, which were then stripped and re-probed with a mouse anti-β-actin monoclonal antibody. The intensity of the immunoreactive bands was estimated by optical density measurements of scanned images using Image J (NIH, Bethesda, MD), a public domain JAVA image-processing program. Columns are means means ± SEM of three independent experiments, whereas the immunoblot is representative of one of these experiments.

G_q-proteins (Figure 6B). In the presence of 1 μM Q109, the PAR_1-AP concentration–response curve was not significantly shifted to the right, but the E_{max} value was reduced (71.0 ± 4.9%; $n = 3$) (Figure 7A; Table 1). The addition of 10 μM Q109 caused a rightward shift in the PAR_1-AP concentration–response curve, resulting in a twofold increase in the EC_{50} value and a 37% reduction in the agonist maximal response (Table 1). As with Q94, the concentration–response curve for PAR_2-AP-induced intracellular Ca^{2+} mobilization was not affected by either 1 or 10 μM Q109 (Figure 7B), indicating that this benzimidazole derivative is a selective negative modulator of PAR_1- but not PAR_2-activated signalling.

Modulation of thrombin-stimulated IP_3 production by benzimidazole derivatives

G_q-coupled receptors, including PAR_1, induce an increase in intracellular Ca^{2+} that occurs secondary to IP_3 production. Therefore, the effects of Q94 and Q109 were evaluated using thrombin-induced IP_3 production, a signalling event closer to receptor activation. Thrombin induced an increase in IP_3

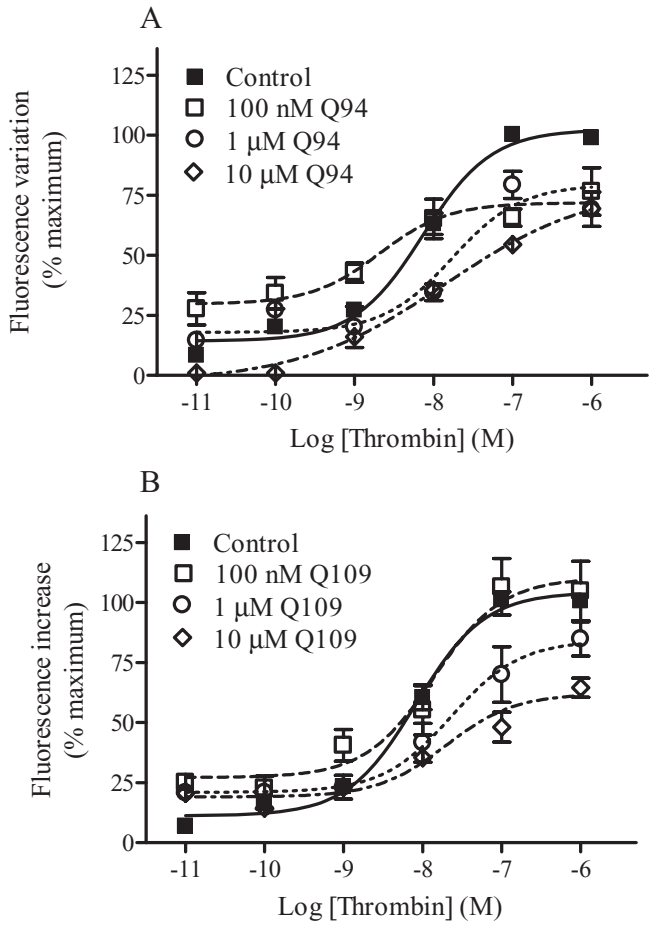

Figure 3

Modulation of thrombin-induced intracellular Ca^{2+} mobilization by Q94 (A) and Q109 (B). Intracellular Ca^{2+} mobilization was measured using Fluo 3-AM-loaded HMECs-1 as described in Methods. Basal $[Ca^{2+}]_i$ was 240.1 ± 45.3 nM (n = 4). The benzimidazole compounds were added 15 min before the addition of thrombin. The concentration–response curves were performed using seven different concentrations of the enzyme in the presence and absence of fixed concentrations of PAR_1 modulators. Data are reported as % of maximal RF and are the means ± SEM of three (A) and four (B) independent experiments, each performed in triplicate.

levels in HMECs-1 in a concentration-dependent manner (Figure 8), with an EC_{50} value of 6.6 ± 1.5 nM (n = 3), while 100 nM thrombin maximally induced IP_3 production. A good correlation was obtained between thrombin-induced $[Ca^{2+}]_i$ increase and IP_3 production, as shown by a comparison of the concentration–response curves (Figure 1A and Figure 8). Consistent with our Ca^{2+} results, micromolar concentrations of either Q94 or Q109 caused a reduction of thrombin-induced IP_3 production (Figure 8), as shown by the rightwards shift of the concentration–response curves and significant decrease in E_{max} value (Table 2). These results indicate that the benzimidazole derivatives interfere with PAR_1-induced G_q activation and signalling.

Modulation of PAR_1-induced inhibition of FSK- or isoprenaline-stimulated cAMP production by benzimidazole derivatives

As we intended to analyse the effect of the benzimidazole derivatives on PAR_1 signalling through $G_{i/o}$-proteins in intact cells, various experimental approaches and conditions to measure thrombin-mediated inhibition of cAMP production induced by either FSK or isoprenaline in HMECs-1 were tested. Using the cAMP detection system described in Methods, we were able to measure robust PAR_1-mediated inhibition of cAMP accumulation in HMECs-1 (Figure 9). Cell stimulation with either 0.5 μM FSK or 1 μM isoprenaline provided a consistent increase in cAMP production, while thrombin significantly inhibited such production in a concentration-dependent fashion (Figure 9A and B). Thrombin at a concentration of 5 nM inhibited both FSK- and isoprenaline-stimulated cAMP production by ~50%, while at 50 nM thrombin, the inhibitory effect was ~90% of maximal inhibition. Concentrations of the benzimidazole derivatives ranging from 100 nM to 10 μM were unable to reverse the inhibitory effect of either 5 or 50 nM thrombin on stimulated cAMP accumulation (Figure 9A and B).

Unexpectedly, we noted that in the absence of thrombin, the presence of either Q94 or Q109 (10 μM) resulted in a ~20–30% inhibition of FSK- or isoprenaline-stimulated cAMP production. This unanticipated result raises the question of whether the benzimidazole compounds might be acting directly on AC, as this effect was evident on both FSK- and isoprenaline-stimulated cAMP production. In order to better understand the action of Q94 and Q109 with respect to $G_{i/o}$ signalling, HMECs-1 were treated with PTX overnight to induce ADP-ribosylation of $G\alpha_{i/o}$ subunits and thus block PAR_1 signalling to $G_{i/o}$-proteins. In PTX-treated cells, 50 nM thrombin caused a ~29% inhibition of FSK-stimulated cAMP production, while in untreated cells, the inhibitory effect reached ~80% (Figure 10). The significant inhibitory effect of Q109 on FSK-stimulated cAMP production in untreated cells was not observed in PTX-treated HMECs-1 (Figure 10), indicating this effect is mediated through $G_{i/o}$. However, the effects observed with Q94 on cAMP production are more difficult to interpret. Even though the inhibitory effect observed with 10 μM Q94 on FSK-stimulated cAMP production was reduced (~20% in PTX-treated cells as compared with the ~40% obtained in parallel experiments in untreated cells; Figure 10), the inhibition was still significant (P < 0.01).

Discussion

Since the initial identification that multiple PARs exist, many physiological and pathophysiological events have been ascribed to their cellular signalling. The involvement of PARs in various processes and their complex interplay has stimulated researchers to develop receptor antagonists not only as tools for pharmacological characterization but more significantly as therapeutic approaches. Numerous peptide, peptidomimetic and non-peptide PAR_1 antagonists are now available for both experimental studies and pharmaceutical use in humans (Chackalamannil, 2006; Ramachandran and Hollenberg, 2008). Many non-peptide antagonists appear to

Table 1

Effects of benzimidazole compounds on parameters of agonist-induced intracellular Ca^{2+} mobilization

	Thrombin EC_{50} (nM)	E_{max} (%)	PAR_1-AP EC_{50} (μM)	E_{max} (%)	PAR_2-AP EC_{50} (μM)	E_{max} (%)
Control	8.4 ± 0.8 (n = 4)	109.3 ± 3.8	6.8 ± 0.8 (n = 6)	100.1 ± 3.4	11.4 ± 0.8 (n = 6)	102.5 ± 4.0
+100 nM Q94	2.1 ± 0.5 (n = 3)***	71.9 ± 4.8**	n.d.	n.d.	n.d.	n.d.
+1 μM Q94	16.9 ± 0.5 (n = 3)***	79.4 ± 6.8**	13.3 ± 0.8 (n = 3)***	94.2 ± 4.5	9.5 ± 0.8 (n = 3)	101.6 ± 4.8
+10 μM Q94	14.0 ± 0.8 (n = 3)***	78.8 ± 6.4**	15.2 ± 0.7 (n = 3)***	72.1 ± 4.7**	9.3 ± 0.8 (n = 3)	109.4 ± 4.6
+100 nM Q109	13.8 ± 0.6 (n = 4)***	110.2 ± 7.5	n.d.	n.d.	n.d.	n.d.
+1 μM Q109	23.1 ± 0.6 (n = 4)***	84.2 ± 7.4*	4.3 ± 0.6 (n = 3)	71.0 ± 4.9**	11.3 ± 0.8 (n = 3)	100.0 ± 3.2
+10 μM Q109	19.9 ± 0.7 (n = 4)***	62.0 ± 2.6***	14.6 ± 0.5 (n = 3)***	62.9 ± 5.8***	13.9 ± 0.8 (n = 3)	101.8 ± 4.9
+10 μM Q89	2.5 ± 0.3 (n = 3)***	101.6 ± 3.1	n.d.	n.d.	n.d.	n.d.

EC_{50} and E_{max} values were obtained by fitting concentration–response curves of Figures 1, 2, 3, 5 and 6 using the non-linear regression analysis of GraphPad Prism version 4.00 for Windows. E_{max} is expressed as % of maximal RF (RF = (F_s – F_0) / F_0, where F_0 is basal fluorescence, and F_s fluorescence recorded after cell stimulation with the agonist). Data are means ± SEM of values from at least three independent experiments performed in triplicate. *P < 0.05; **P < 0.01; ***P < 0.001, significantly different from corresponding control by ANOVA followed by Bonferroni's multiple comparison test.
n.d., not determined.

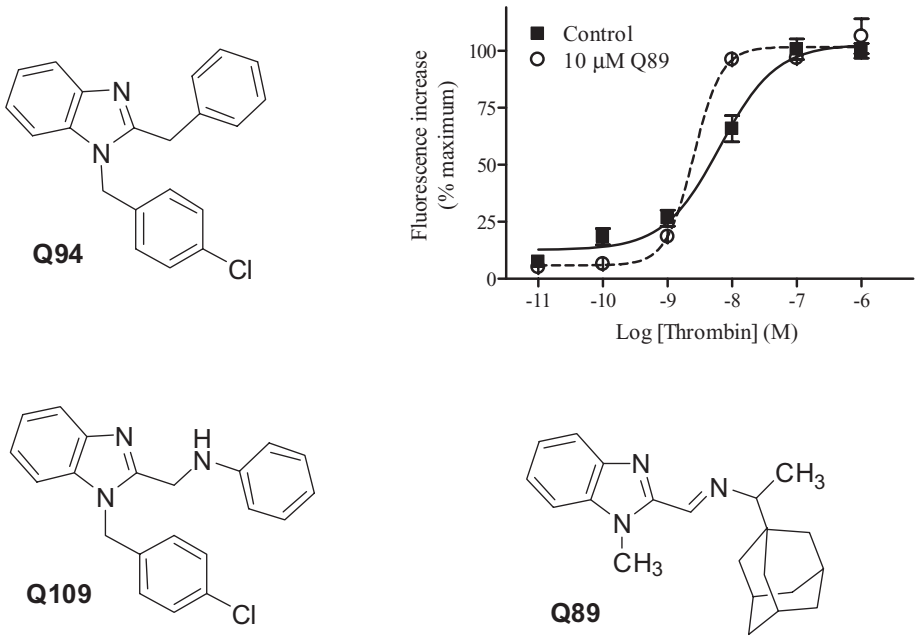

Figure 4

Molecular structures of the benzimidazole derivatives and effect (inset) of an analogue, Q89, on thrombin-induced intracellular Ca^{2+} mobilization. Intracellular Ca^{2+} mobilization was measured using Fluo 3-AM-loaded HMECs-1 as described in Methods. Basal $[Ca^{2+}]_i$ was 232.3 ± 40.2 nM (n = 3). The benzimidazole compound Q89 was added 15 min before the addition of thrombin. The concentration–response curves were performed using seven different concentrations of the enzyme in the presence and absence of 10 μM Q89. Data are reported as % of maximal RF and are the means ± SEM of three experiments, each performed in triplicate.

be effective antithrombotic agents in humans (Chackalamannil *et al.*, 2005; Chackalamannil, 2006), although to date none have received FDA approval (Sugunaraj *et al.*, 2011).

The possibility of modulating PAR_1 activation through allosteric modulation using non-peptide molecules has been poorly explored. Recently, Dowal *et al.* (2011) identified an analogue of 1,2,3,4-tetrahydro-4-pentyl-9*H*-cyclopenta[b] quinolin-9-imine, JF5, as an allosteric modulator of PAR_1. The use of a benzimidazole derivative, Q94, to specifically block PAR_1 signalling mediated by G_q-proteins was initially reported by Deng *et al.* (2008) and then later confirmed (Scotton *et al.*, 2009). This compound was originally identified during an

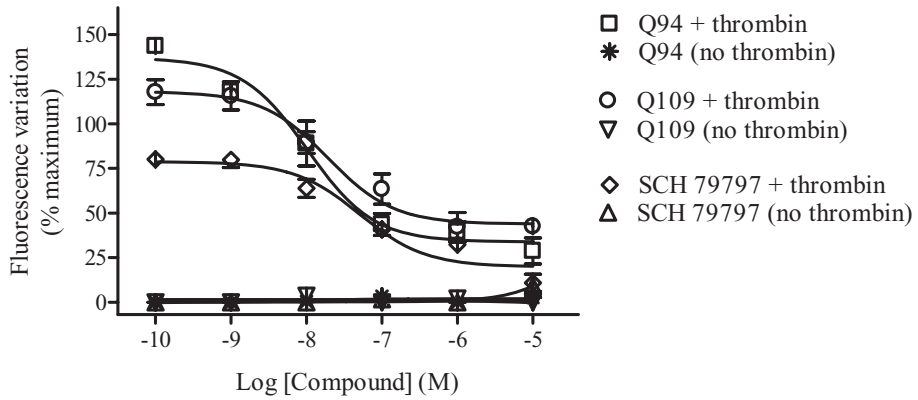

Figure 5

Concentration-dependent inhibition of thrombin-induced intracellular Ca^{2+} mobilization by Q94, Q109 and SCH 79797. Intracellular Ca^{2+} mobilization was measured using Fluo 3-AM-loaded HMECs-1 as described in Methods. Basal $[Ca^{2+}]_i$ was 250.1 ± 32.0 nM ($n = 3$). The concentration–response curves were carried out using 6 different concentrations of the compounds in the presence and absence of 50 nM thrombin. Thrombin was added 15 min after the addition of compounds. Data are reported as % of maximal RF and are the means ± SEM of three experiments, each performed in triplicate.

Table 2

Effect of benzimidazole compounds on thrombin's maximal stimulation of IP_3 production

	E_{max} (pmol per well)
Control	242.0 ± 22.1
+1 μM Q94	118.1 ± 7.5***
+10 μM Q94	111.0 ± 6.0***
+1 μM Q109	153.0 ± 11.0*
+10 μM Q109	104.2 ± 6.1***

E_{max} values were obtained by fitting concentration–response curves of three independent using the non-linear regression analysis of GraphPad Prism version 4.00 for Windows Data are means ± SEM of values from three independent experiments performed in triplicate. *$P < 0.05$; ***$P < 0.001$, significantly different from corresponding control by ANOVA followed by Bonferroni's multiple comparison test.

ELISA screen that identified hits based on their ability to compete with a high-affinity peptide mimicking the C-terminus of $G\alpha_q$ (Deng *et al.*, 2008) and probably represents a new class of negative modulators of PAR_1 signalling.

We investigated the pharmacological activity and specificity of three benzimidazole derivatives (Q94, Q109, Q89) utilizing PAR_1 endogenously expressed in HMECs-1 and identified Q94 and Q109 as effective negative modulators of PAR_1-activated G_q signalling. Compound Q94 appears to be twofold more potent than Q109 at inhibiting thrombin-induced intracellular Ca^{2+} mobilization, while the analogue Q89 is devoid of any inhibitory activity. From a structural point of view, all three compounds possess the same benzimidazole scaffold, but Q89 substituents are quite different from those of Q94 and Q109, which present some similarities. The benzimidazole nucleus of both Q94 and Q109 bears substituents of similar characteristic in terms of lipophilicity and steric hindrance at 1- and 2-positions. In contrast, Q89 possesses a small methyl group at the 1-position and a very bulky lipophilic adamantane bonded at the 2-position through a linker of limited flexibility. This bulky moiety with reduced movement ability may interfere with a suitable fitting of Q89 on the receptor interaction site, while the two lipophilic substituents of Q94 and Q109 may contribute to a more efficacious interaction with the receptor. The slight reduction in potency displayed by Q109 on thrombin-mediated responses may be due to the length of the linker between the benzimidazole nucleus and the phenyl ring of the substituent at 2-position. A commercially available pyrroloquinazoline compound, SCH 79797 (Ahn *et al.*, 2000), which is considered to be a selective PAR_1-competitive antagonist, also inhibited thrombin-stimulated intracellular Ca^{2+} mobilization in our assay system, but it was five- and approximately threefold less potent than Q94 and Q109, respectively.

A series of benzimidazole derivatives have been previously reported to be high-affinity PAR_1 antagonists with the ability to potently inhibit thrombin-induced platelet aggregation (Chackalamannil *et al.*, 2001). However, the compounds were 1,3-disubstituted benzimidazole derivatives, while our compounds are 1,2-disubstituted benzimidazole derivatives. Nevertheless, both types of compound require at least a benzyl group as a substituent at N to exert the optimal inhibitory activity. Chackalamannil *et al.* (2005) showed that the 1,3-disubstituted benzimidazole derivatives were competitive inhibitors of [^{125}I]-TRAP binding to PAR_1. However, as allosteric modulators can mimic orthosteric antagonists and alter ligand binding (Christopoulos and Kenakin, 2002), without the benefit of dissociation rate kinetics, we can only speculate that the 1,3-disubstituted bezimidazole derivatives may indeed be negative allosteric modulators.

The present study provides the first characterization of two 1,2-disubstituted bezimidazole derivatives, Q94 and Q109, as possible negative allosteric modulators of PAR_1 G_q

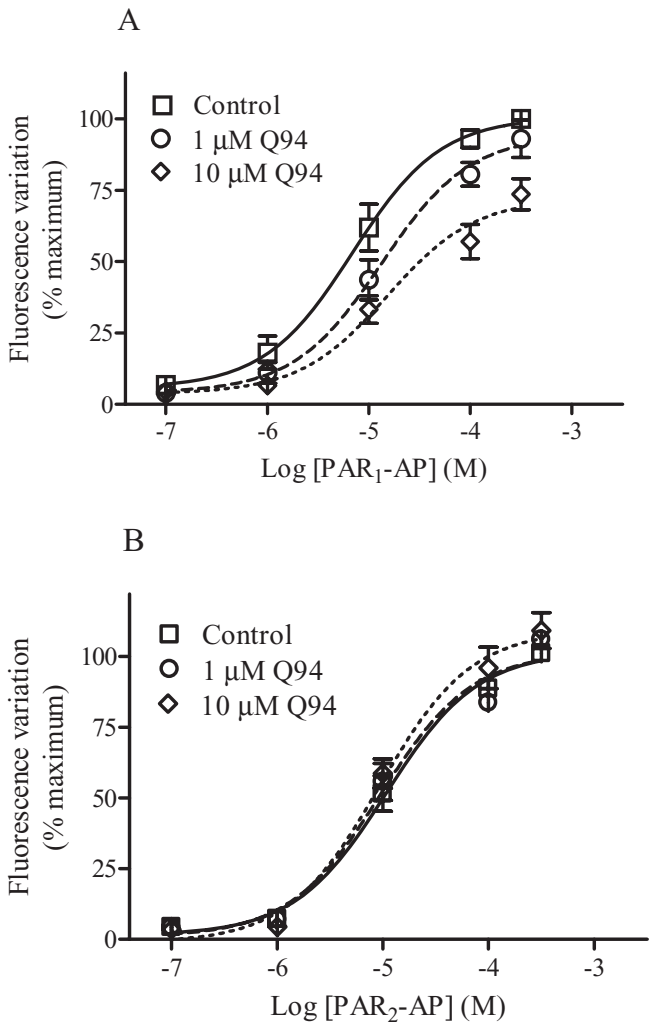

Figure 6

Modulation of (A) PAR_1-AP- and (B) PAR_2-AP-induced intracellular Ca^{2+} mobilization by Q94. Intracellular Ca^{2+} mobilization was measured using Fluo 3-AM-loaded HMECs-1 as described in Methods. Basal $[Ca^{2+}]_i$ was 210.5 ± 35.8 nM ($n = 3$). The concentration–response curves were performed using five different concentrations of the agonist peptides in the presence and absence of two fixed concentrations of Q94 added 15 min before the addition of PAR_1-AP (A) or PAR_2-AP (B). Data are reported as % of maximal RF and are the means ± SEM of three experiments, each performed in triplicate.

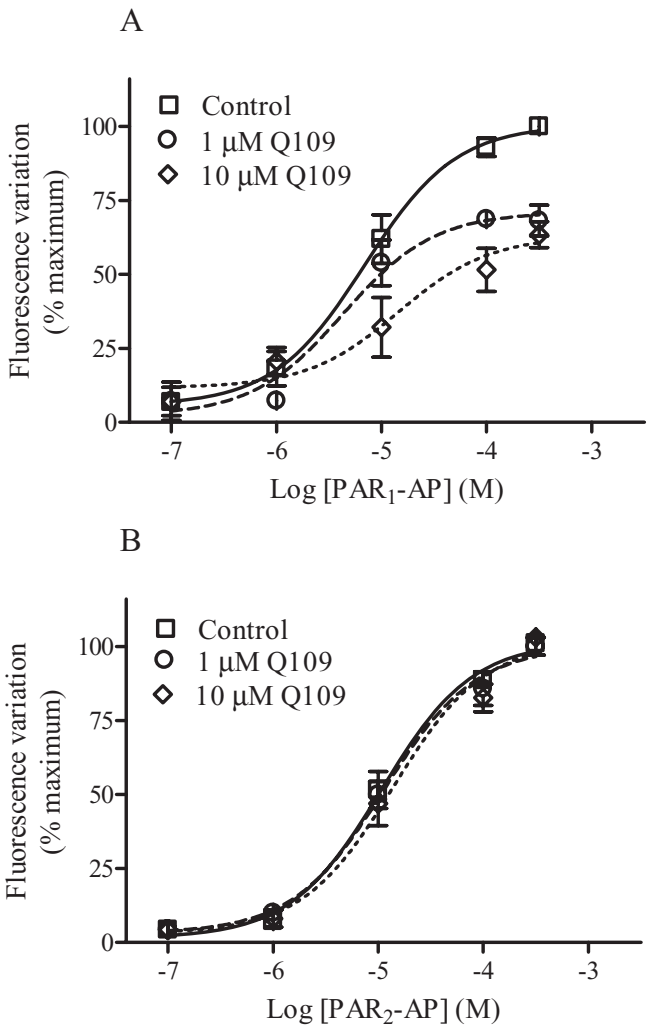

Figure 7

Modulation of (A) PAR_1-AP- and (B) PAR_2-AP-induced intracellular Ca^{2+} mobilization by Q109. Intracellular Ca^{2+} mobilization was measured using Fluo 3-AM-loaded HMECs-1 as described in Methods. Basal $[Ca^{2+}]_i$ was 290.1 ± 51.2 nM ($n = 3$). The concentration–response curves were performed using five different concentrations of the agonist peptides in the presence and absence of two fixed concentrations of Q109 added 15 min before the addition of PAR_1-AP (A) or PAR_2-AP (B). Data are reported as % of maximal RF and are the means ± SEM of three experiments, each performed in triplicate.

signalling. When tested in biochemical functional assays (Ca^{2+}, IP_3), which are indirect measures of PAR_1-induced activation of G_q-proteins, increasing concentrations of the benzimidazole derivatives caused a progressive shift to the right and a decrease in the maximal response of agonist (thrombin or PAR_1-AP) concentration–response curves. These findings are in agreement with proposed simulations of allosterism in functional assays (Ehlert, 2005; Kenakin and Miller, 2010) and indicate that there is little receptor reserve. However, at a concentration of 100 nM, both compounds caused an additive effect on intracellular Ca^{2+} mobilization induced by 1 pM to 1 nM thrombin. Interestingly, the positive modulation of Q94 at 100 nM concentrations was accompanied by a reduction in Ca^{2+} mobilization at higher levels of thrombin, and a marked decrease in the E_{max} response. As Q94 and Q109 did not affect basal probe fluorescence (Figure 4), we conclude that Q94 behaves differently depending on its concentration, as well as that of thrombin.

Is this hypothesis in agreement with the theoretical basis of allosteric modulator effects? We must consider that PAR_1 couples to multiple G-proteins, $G_{q/11}$, $G_{i/o}$ and $G_{12/13}$ (Ramachandran and Hollenberg, 2008; Russo *et al.*, 2009) and the existence of distinct active receptor conformations is supported by the demonstration of ligand-induced biased signalling by thrombin versus PAR_1-AP, with thrombin favouring $G_{12/13}$ signalling, while PAR_1-AP primarily initiates G_q signalling (McLaughlin *et al.*, 2005; Russo *et al.*, 2009). Moreover,

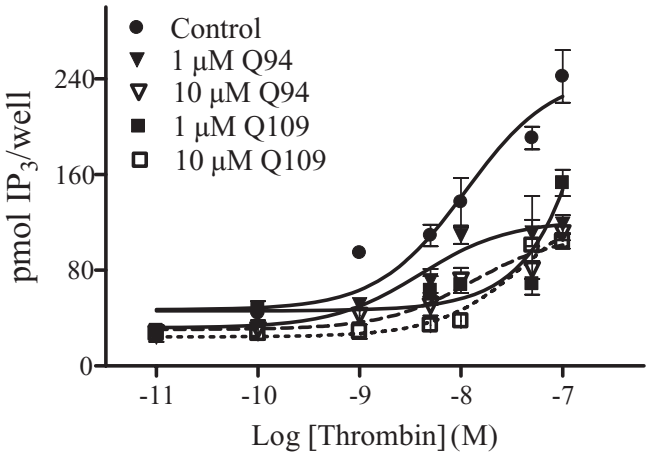

Figure 8

Effect of Q94 and Q109 on thrombin-induced IP_3 production. Accumulation of IP_3 in HMECs-1 was measured using a competitive protein binding method as described in Methods. Cells were stimulated with different concentrations of thrombin in the presence and absence of two different concentrations (1 or 10 μM) of Q94 or Q109 as described in Methods. In the absence of thrombin, compounds did not cause any change in IP_3 production. Values are the means ± SEM of triplicate results from one experiment performed two additional times with similar results.

there is a recent report of an allosteric PAR_1 inhibitor, JF5, that can selectively modulate PAR_1 signalling through G_{12} but not G_q (Dowal *et al.*, 2011). Thus, binding of Q94 to its allosteric site may stabilize a receptor conformation, which is not favourable to G_q activation but rather favours G_i interaction and activation. If this were the case, the effect on PAR_1 signalling would result in (a) disruption of $G\alpha_q$ signalling to PLC_β and therefore decrease in intracellular Ca^{2+} mobilization and (b) preferential activation of G_i-proteins, which activate PLC_β through $G\beta\gamma$. The balance between these contrasting effects may be responsible for the observed shape of the thrombin concentration–response curve in the presence of 100 nM Q94. It is worth mentioning that Vanhauwe *et al.*, (2002) reported that in HMECs-1 G_o-proteins play a role in thrombin signalling, specifically Ca^{2+} mobilization, through their $G\beta\gamma$ subunits. Contrary to this, McLaughlin *et al.*, (2005) presented results that seem to exclude the involvement of G_i- and G_o-proteins (PTX-inhibited G-proteins) in thrombin-induced Ca^{2+} mobilization in HMECs-1. These differences may arise from the use of different techniques to measure intracellular Ca^{2+} response, namely single cell fluorescence recording (Vanhauwe *et al.*, 2002) and cell layer fluorescence measurement (McLaughlin *et al.*, 2005).

We demonstrated that both Q94 and Q109 are PAR_1 subtype selective as neither compound altered PAR_2 signalling, as measured by Ca^{2+} mobilization, in HMECs-1. However, while both Q94 and Q109 affected the PAR_1-AP concentration–response curve, their modulatory effects were not identical to those observed with thrombin. Specifically, 1 μM Q94 resulted in a significant increase in EC_{50} and no change to the E_{max} with PAR_1-AP, while 1 μM Q109 resulted in a small reduction in the EC_{50} and a significant reduction in E_{max}. Studies by Ayoub *et al.* (2010), using bioluminescence resonance energy transfer and time-resolved fluorescence resonance energy transfer, revealed PAR_1 forms pre-assembled complexes with G_i independent of thrombin stimulation. Therefore, it is tempting to speculate that the differences between the effects of Q109 and Q94 on PAR_1-AP-induced Ca^{2+} mobilization reflect distinct receptor conformations that allow pre-coupling to different G-proteins (G_i, G_q, G_{12}).

Since PAR_1-induced variations in $[Ca^{2+}]_i$ result as a consequence of intracellular Ca^{2+} mobilization from the endoplasmic reticulum and Ca^{2+} entry from the extracellular milieu into endothelial cells (Vandenbroucke *et al.*, 2008; Dietrich *et al.*, 2010), we also analysed the ability of Q94 and Q109 to inhibit thrombin-induced IP_3 production. Indeed, micromolar concentrations of the compounds displayed an inhibitory effect on thrombin-mediated IP_3 accumulation, indicating that they act by disrupting PAR_1 G_q activation and downstream signalling events. Both compounds caused significant decreases in the thrombin E_{max} value, suggesting they act as negative allosteric modulators of PAR_1 rather than competitive antagonists.

Finally, our experiments provide evidence that the 1,2-disubstituted benzimidazole derivatives positively modulate PAR_1 G_i coupling. Whereas Q94 and Q109 do not modify thrombin-induced inhibition of either FSK- or isoprenaline-stimulated cAMP production in HMECs-1, in the absence of thrombin, they both inhibited cAMP accumulation. This unexpected observation suggests that Q94 and Q109 may stabilize a PAR_1 conformation favouring G_i activation. Cell treatment with PTX served to demonstrate that Q109 inhibition of FSK-stimulated cAMP production was mediated through G_i activation. The interaction of Q109 with PAR_1 probably induces a receptor conformation that favours coupling and activation of G_i-proteins, even in the absence of the agonist. This hypothesis seems to be supported by recent work that revealed PAR_1 forms pre-assembled complexes with $G\alpha_{i1}$ rather than $G\alpha_{12}$ (Ayoub *et al.*, 2010). Thus, it appears that Q109 can be considered an 'allosteric agonist' of PAR_1 G_i signalling (Wang *et al.*, 2009). Allosteric agonists have been described for several GPCRs including the glucagon-like peptide 1 receptor (Christopoulos and Kenakin, 2002; Knudsen *et al.*, 2007). However, unlike typical 'allosteric agonists', Q109 also seems to behave as a negative allosteric modulator of PAR_1 G_q signalling. The pharmacology underlying Q94 is complicated, as in PTX-treated cells, although the inhibition of FSK-stimulated cAMP production was reduced, it was still detectable. As a result, we cannot exclude an off-target effect of Q94, produced via an interaction with AC. Indeed, there are many examples of allosteric modulating agents that possess other significant pharmacological functions (Wang *et al.*, 2009).

In conclusion, we demonstrated that both Q94 and Q109 act as selective negative modulators of PAR_1 G_q signalling. Our investigation suggests that in addition to their negative modulation of PAR_1 G_q signalling, these 1,2-disubstituted benzimidazole derivatives also act as positive allosteric agonists of PAR_1 G_i signalling. The recently identified allosteric modulator of PAR_1, JF5 (Dowal *et al.*, 2011), also shows selectivity for $G\alpha$ subunits, blocking signalling through G_q but not G_{12}. Allosteric ligands possess specific advantages over classical orthosteric ligands and may help in the development of

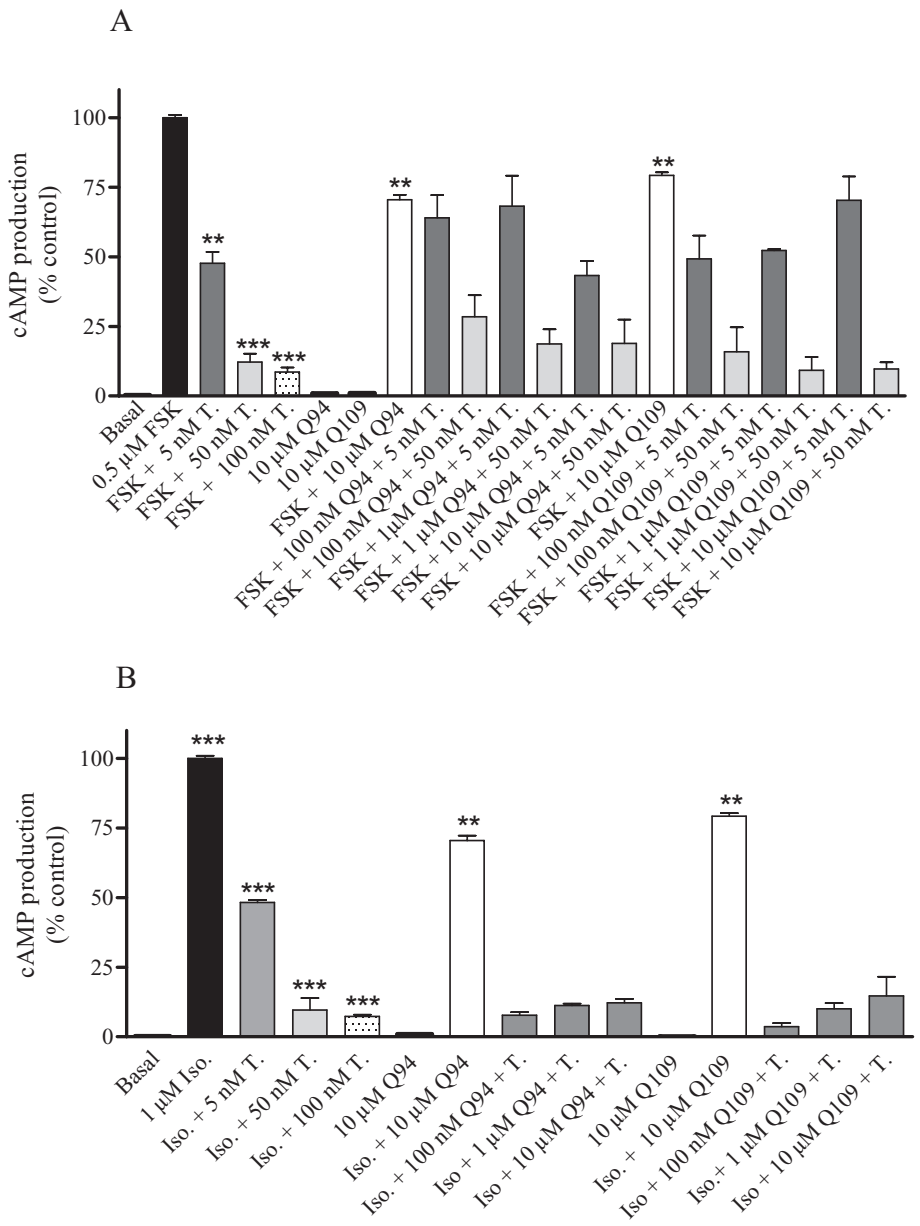

Figure 9

Effect of Q94 and Q109 on thrombin (T)-induced inhibition of (A) FSK- and (B) isoprenaline (Iso)-stimulated cAMP accumulation. Production of cAMP in HMECs-1 was measured using a competition binding assay that includes the bovine adrenal cAMP binding protein and [^{3}H]-cAMP as described in Methods. Cells, exposed for 15 min to Q94 or Q109, in the presence or absence of 5 or 50 nM thrombin were treated with 0.5 µM FSK (A) or 1 µM (B) isoprenaline. Basal value was 1.0 ± 0.1 pmol per well, while FSK and isoprenaline stimulation induced cAMP accumulation of 66.0 ± 5.9 and 189.0 ± 10.5 pmol per well, respectively. Values are the means ± SEM of three experiments, each performed in duplicate. **, $P < 0.01$; ***, $P < 0.001$ indicates values that are significantly different from FSK- or isoprenaline-stimulated value, as determined by Student's unpaired *t* test.

therapeutic agents that are not only receptor-subtype selective but also signalling pathway selective (Christopoulos and Kenakin, 2002). Our studies, while not resulting in the definition of either Q94 or Q109 as potent drug-like structures, do represent a starting point for development of dual signalling pathway-selective positive/negative modulators of PAR_1.

Acknowledgements

We thank Drs HE Hamm (Department of Pharmacology, Vanderbilt University, Nashville, TN) and F Da Settimo (Department of Pharmaceutical Sciences, University of Pisa, Pisa, Italy) for their helpful discussions. We are grateful to Dr M Luconi (Department of Clinical Physiopathology, University

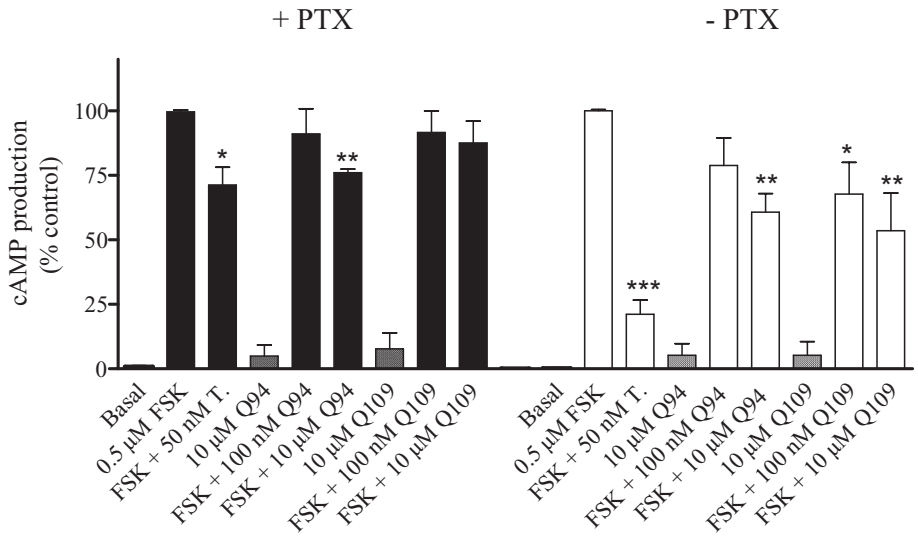

Figure 10

Effect of Q94 and Q109 on thrombin-induced inhibition of FSK-stimulated cAMP accumulation in PTX-treated (A) and untreated (B) HMECs-1. Production of cAMP was measured using a competition binding assay that includes the bovine adrenal cAMP binding protein and [^{3}H]-cAMP as described in Methods. PTX-treated (A) and control (B) HMECs-1 were exposed for 15 min to Q94 or Q109 in the presence and absence of 50 nM thrombin and then stimulated with 0.5 μM FSK. Basal values for treated and control cells were 1.3 ± 0.1 and 1.1 ± 0.1 pmol per well, respectively. FSK stimulation of treated and control cells induced cAMP accumulation of 75.6 ± 1.2 and 69.5 ± 8.9 pmol per well, respectively. Values are the means ± SEM of four experiments, each performed in duplicate. Values that are significantly different (*, $P < 0.05$; **, $P < 0.01$; ***, $P < 0.001$) from FSK-stimulated value as determined by unpaired Student's *t* test are indicated.

of Florence, Italy) for expert advice and support on HMEC-1 culture conditions. This work was supported by grants from 'Ministero dell'Istruzione, dell'Università e della Ricerca' (MIUR) and University of Pisa to MRM.

Conflicts of interest

AG has previously received honoraria for both consultation and speaking at meetings from PerkinElmer, Promega and ThermoFisher.

References

Ades EW, Candal FJ, Swerlick RA, George VG, Summers S, Bosse DC *et al.* (1992). HMEC-1: establishment of an immortalized human microvascular endothelial cell line. J Invest Dermatol 99: 683–690.

Ahn HS, Foster C, Boykow G, Stamford A, Manna M, Graziano M (2000). Inhibition of cellular action of thrombin by N3-cyclopropyl-7-[[4-(1-methylethyl)phenyl]methyl]-7H-pyrrolo[3,2-f]quinazoline-1,3-diamine (SCH 79797), a nonpeptide thrombin receptor antagonist. Biochem Pharmacol 60: 1425–1434.

Alexander SPH, Mathie A, Peters JA (2011). Guide to Receptors and Channels (GRAC), 5th edn. Br J Pharmacol 164 (Suppl. 1): S1–S324.

Ayoub MA, Trinquet E, Pfleger KD, Pin JP (2010). Differential association modes of the thrombin receptor PAR$_1$ with Gα_{i1}, Gα_{12}, and β-arrestin 1. FASEB J 24: 3522–3535.

Barr AJ, Brass LF, Manning DR (1997). Reconstitution of receptors and GTP-binding regulatory proteins (G proteins) in Sf9 cells. A direct evaluation of selectivity in receptor.G protein coupling. J Biol Chem 272: 2223–2229.

Chackalamannil S (2006). Thrombin receptor (protease activated receptor-1) antagonists as potent antithrombotic agents with strong antiplatelet effects. J Med Chem 49: 5389–5403.

Chackalamannil S, Doller D, Eagen K, Czarniecki M, Ahn HS, Foster CJ *et al.* (2001). Potent, low molecular weight thrombin receptor antagonists. Bioorg Med Chem Lett 11: 2851–2853.

Chackalamannil S, Xia Y, Greenlee WJ, Clasby M, Doller D, Tsai H *et al.* (2005). Discovery of potent orally active thrombin receptor (protease activated receptor 1) antagonists as novel antithrombotic agents. J Med Chem 48: 5884–5887.

Christopoulos A, Kenakin T (2002). G protein-coupled receptor allosterism and complexing. Pharmacol Rev 54: 323–374.

Colotta V, Lenzi O, Catarzi D, Varano F, Filacchioni G, Martini C *et al.* (2009). Pyrido[2,3-e]-1,2,4-triazolo[4,3-a]pyrazin-1-one as a new scaffold to develop potent and selective human A$_3$ adenosine receptor antagonists. Synthesis, pharmacological evaluation, and ligand-receptor modeling studies. J Med Chem 52: 2407–2419.

Coughlin SR (2001). Protease-activated receptors in vascular biology. Thromb Haemost 86: 298–307.

Covic L, Gresser AL, Talavera J, Swift S, Kuliopulos A (2002a). Activation and inhibition of G protein-coupled receptors by cell-penetrating membrane-tethered peptides. Proc Natl Acad Sci USA 99: 643–648.

Covic L, Misra M, Badar J, Singh C, Kuliopulos A (2002b). Pepducin-based intervention of thrombin-receptor signaling and systemic platelet activation. Nat Med 8: 1161–1165.

Deng X, Mercer PF, Scotton CJ, Gilchrist A, Chambers RC (2008). Thrombin induces fibroblast CCL2/JE production and release via coupling of PAR_1 to $G\alpha_q$ and cooperation between ERK1/2 and Rho kinase signaling pathways. Mol Biol Cell 19: 2520–2533.

Dietrich A, Kalwa H, Gudermann T (2010). TRPC channels in vascular cell function. Thromb Haemost 103: 262–270.

Dowal L, Sim DS, Dilks JR, Blair P, Beaudry S, Denker BM *et al.* (2011). Identification of an antithrombotic allosteric modulator that acts through helix 8 of PAR_1. Proc Natl Acad Sci USA 108: 2951–2956.

Ehlert FJ (2005). Analysis of allosterism in functional assays. J Pharmacol Exp Ther 315: 740–754.

Fujiwara M, Jin E, Ghazizadeh M, Kawanami O (2005). Activation of PAR_4 induces a distinct actin fiber formation via p38 MAPK in human lung endothelial cells. J Histochem Cytochem 53: 1121–1129.

Gerwins P (1993). Modification of a competitive protein binding assay for determination of inositol 1,4,5-trisphosphate. Anal Biochem 210: 45–49.

Gilchrist A, Vanhauwe JF, Li A, Thomas TO, Voyno-Yasenetskaya T, Hamm HE (2001). Gα minigenes expressing C-terminal peptides serve as specific inhibitor s of thrombin-mediated endothelial activation. J Biol Chem 276: 25672–25679.

Hamilton JR, Moffatt JD, Frauman AG, Cocks TM (2001). Protease-activated receptor (PAR) 1 but not PAR_2 or PAR_4 mediates endothelium-dependent relaxation to thrombin and trypsin in human pulmonary arteries. J Cardiovasc Pharmacol 38: 108–119.

Hamilton JR, Moffatt JD, Tatoulis J, Cocks TM (2002). Enzymatic activation of endothelial protease-activated receptors is dependent on artery diameter in human and porcine isolated coronary arteries. Br J Pharmacol 136: 492–501.

Hirano K, Nomoto N, Hirano M, Momota F, Hanada A, Kanaide H (2007). Distinct Ca^{2+} requirement for NO production between proteinase-activated receptor 1 and 4 (PAR_1 and PAR_4) in vascular endothelial cells. J Pharmacol Exp Ther 322: 668–677.

Hollenberg MD, Compton SJ (2002). International Union of Pharmacology. XXVIII. Proteinase-activated receptors. Pharmacol Rev 54: 203–217.

Kahn ML, Nakanishi-Matsui M, Shapiro MJ, Ishihara H, Coughlin SR (1999). Protease-activated receptors 1 and 4 mediate activation of human platelets by thrombin. J Clin Invest 103: 879–887.

Kenakin T, Miller LJ (2010). Seven transmembrane receptors as shapeshifting proteins: the impact of allosteric modulation and functional selectivity on new drug discovery. Pharmacol Rev 62: 265–304.

Knudsen LB, Kiel D, Teng M, Behrens C, Bhumralkar D, Kodra JT *et al.* (2007). Small-molecule agonists for the glucagon-like peptide 1 receptor. Proc Natl Acad Sci USA 104: 937–942.

Luo W, Wang Y, Reiser G (2007). Protease-activated receptors in the brain: receptor expression, activation, and functions in neurodegeneration and neuroprotection. Brain Res Rev 56: 331–345.

Macfarlane SR, Seatter MJ, Kanke T, Hunter GD, Plevin R (2001). Proteinase-activated receptors. Pharmacol Rev 53: 245–282.

McLaughlin JN, Shen L, Holinstat M, Brooks JD, Dibenedetto E, Hamm HE (2005). Functional selectivity of G protein signaling by agonist peptides and thrombin for the protease-activated receptor-1. J Biol Chem 280: 25048–25059.

Nordstedt C, Fredholm BB (1990). A modification of a protein-binding method for rapid quantification of cAMP in cell-culture supernatants and body fluid. Anal Biochem 189: 231–234.

Nystedt S, Emilsson K, Larsson AK, Strömbeck B, Sundelin J (1995). Molecular cloning and functional expression of the gene encoding the human proteinase-activated receptor 2. Eur J Biochem 232: 84–89.

O'Brien PJ, Prevost N, Molino M, Hollinger MK, Woolkalis MJ, Woulfe DS *et al.* (2000). Thrombin responses in human endothelial cells. Contributions from receptors other than PAR_1 include the transactivation of PAR_2 by thrombin-cleaved PAR_1. J Biol Chem 275: 13502–13509.

Ramachandran R, Hollenberg MD (2008). Proteinases and signaling: pathophysiological and therapeutic implications via PARs and more. Br J Pharmacol 153: S263–S282.

Ramachandran R, Mihara K, Mathur M, Rochdi MD, Bouvier M, Defea K *et al.* (2009). Agonist-biased signaling via proteinase activated receptor-2: differential activation of calcium and mitogen-activated protein kinase pathways. Mol Pharmacol 76: 791–801.

Robin J, Kharbanda R, Mclean P, Campbell R, Vallance P (2003). Protease-activated receptor 2-mediated vasodilatation in humans in vivo: role of nitric oxide and prostanoids. Circulation 107: 954–959.

Russo A, Soh UJ, Trejo J (2009). Proteases display biased agonism at protease-activated receptors: location matters! Mol Interv 9: 87–96.

Scotton CJ, Krupiczojc MA, Königshoff M, Mercer PF, Lee YC, Kaminski N *et al.* (2009). Increased local expression of coagulation factor X contributes to the fibrotic response in human and murine lung injury. J Clin Invest 119: 2550–2563.

Sugunaraj JP, Mehta V, Kalra A, Sukhija R, Palaniswamy C (2011). Protease-Activated Receptor-1 Antagonists: focus on SCH 530348. Am J Ther Jan 18. DOI: 10.1097/MJT.0b013e3181ff7c16 [Epub ahead of print].

Vandenbroucke E, Mehta D, Minshall E, Malik AB (2008). Regulation of endothelial junctional permeability. Ann NY Acad Sci 1123: 134–145.

Vanhauwe JF, Thomas TO, Minshall RD, Tiruppathi C, Li A, Gilchrist A *et al.* (2002). Thrombin receptors activate G_o proteins in endothelial cells to regulate intracellular calcium and cell shape changes. J Biol Chem 277: 34143–34149.

Wang L, Martin B, Brenneman R, Luttrell LM, Maudsley S (2009). Allosteric modulators of G protein-coupled receptors: future therapeutics for complex physiological disorders. J Pharmacol Exp Ther 331: 340–348.

Supporting information

Additional Supporting Information may be found in the online version of this article:

Data S1 Initially, we screened a library of ~10 000 compound obtained from ChemDiv for their ability to compete for binding at PAR_1 with a high-affinity receptor binding peptide probe (HABP) designed around the C-terminus of $G\alpha_q$ (LQLNLKEYNLV). The HABP probe T2-14 (LQLNLKKYNRV)

was identified using a peptide on plasmids approach as previously described (Gilchrist, A, Li, A, Hamm, HE. *Meth. Enzym*. 2000 315:388–404). Briefly, a library of peptides was constructed by sequential substitution of the 11 native C-terminal $G\alpha_q$ amino acids with each of the 20 known amino acids. This peptide library was fused with *Escherichia coli* maltose-binding protein (MBP), to enable recognition by using ELISA. IC_{50} values for binding of MBP_G_q or MBP_T2-14 to activated PAR_1 indicated MBP_T2-14 (106 nM) had a higher binding affinity than did MBP_G_q (320 nM). Initial screening for all compounds was done at 10 μM, followed up by dose–response curves on select compounds. Using this methodology, we found that Q89 was found to compete with MBP_T2-14 for binding to activated PAR_1 receptors with an IC_{50} of 310 nM (Supplementary Figure S1). We identified several commercially available analogs for Q89, including Q94 and Q109, that when tested by ELISA were also found to inhibit binding of MBP_T2-14 to activated PAR_1 receptors with IC_{50} values of 923 and 817 nM respectively.

Figure S1 PAR_1 receptors expressed in membranes of SF9 cells were treated with 100 nM TRAP (thrombin receptor activating peptide). Purified T2-14 fused with *E. coli* maltose-binding protein (MBP-T2-14) at a concentration of 100 nM was added to wells and allowed to bind to the receptor. Increasing amounts of each compound were added to wells in triplicate, and binding of MBP-T2-14 was measured using an ELISA for MBP. Data presented are the mean of individual wells from three separate experiments. A non-linear regression analysis was generated using GraphPad Prism, version 5.0.

Please note: Wiley-Blackwell are not responsible for the content or functionality of any supporting materials supplied by the authors. Any queries (other than missing material) should be directed to the corresponding author for the article.